AD-A171 583 FUNDAMENTAL STUDIES IN THE MOLECULAR BASIS OF LASER INDUCED RETINAL DAMAGE(U) CORNELL UNIV ITHACA NY A LEWIS SEP 83 DAMD17-79-C-9041 1/1

UNCLASSIFIED F/G 6/18 NL

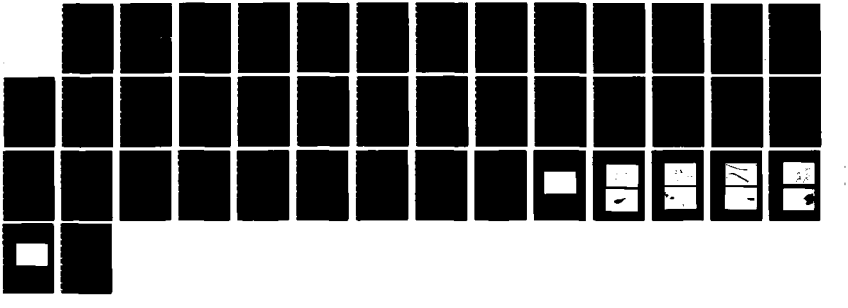

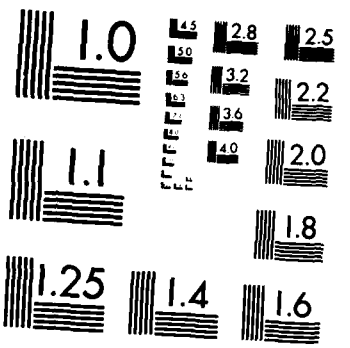

Annual Report

Contract Number: DAMD 17-79-C-9041

Name of Contractor: Cornell University
Ithaca, NY 14853
Principal Investigator: Aaron Lewis

September 1983

Supported by:
US ARMY MEDICAL RESEARCH AND DEVELOPMENT COMMAND
Fort Detrick, Frederick, Maryland 21701-5012

Fundamental Studies in the Molecular Basis of Laser Induced Retinal Damage

SECURITY CLASSIFICATION OF THIS PAGE (When Data Entered)

REPORT DOCUMENTATION PAGE

READ INSTRUCTIONS BEFORE COMPLETING FORM

1. REPORT NUMBER	2. GOVT ACCESSION NO. / 3. RECIPIENT'S CATALOG NUMBER
4. TITLE (and Subtitle): Fundamental Studies in the Molecular Basis of Laser Induced Retinal Damage	5. TYPE OF REPORT & PERIOD COVERED: Annual, Sep 82 - Aug 83
	6. PERFORMING ORG. REPORT NUMBER
7. AUTHOR(s): Aaron Lewis	8. CONTRACT OR GRANT NUMBER(s): DAMD17-79-C-9041
9. PERFORMING ORGANIZATION NAME AND ADDRESS: Cornell University, Ithaca, NY 14853	10. PROGRAM ELEMENT, PROJECT, TASK AREA & WORK UNIT NUMBERS
11. CONTROLLING OFFICE NAME AND ADDRESS: US Army Medical Research and Development Command, Fort Detrick, Frederick, MD 21701	12. REPORT DATE: September 1983
	13. NUMBER OF PAGES: 41
14. MONITORING AGENCY NAME & ADDRESS(if different from Controlling Office)	15. SECURITY CLASS. (of this report)
	15a. DECLASSIFICATION/DOWNGRADING SCHEDULE

16. DISTRIBUTION STATEMENT (of this Report)

Approved for public release; distribution unlimited

17. DISTRIBUTION STATEMENT (of the abstract entered in Block 20, if different from Report)

18. SUPPLEMENTARY NOTES

19. KEY WORDS (Continue on reverse side if necessary and identify by block number)

20. ABSTRACT (Continue on reverse side if necessary and identify by block number)

DD FORM 1 JAN 73 1473 EDITION OF 1 NOV 65 IS OBSOLETE

SECURITY CLASSIFICATION OF THIS PAGE (When Data Entered)

I. General Overview

In this annual report we describe the experimental details behind some of the most significant developments that have occurred in our laboratory during the past year with the support of the U. S. Army. In summary our research has led to major discoveries in two general areas. First, we have been able to show that there are a series of anionic activators of visual cells. These anionic activators turn on, in the dark, the enzymatic processes which are usually stimulated by light. Among these anionic activators is fluoride, the important additive in dental care. It is possible that our discovery of anionic activators will allow us to modulate visual sensitivity and excitation.

A second major advance during the past year has been the development of a staining method which allows the direct observation with light microscopy of actin filaments in rod outer segments. This discovery will now allow us to view these important actin filaments in live cells under physiologically relevant experimental conditions. It will also allow for the development of new methods to probe pathological and damaged conditions in visual photoreceptor cells.

The above discoveries will now be described in two separate sections. The first entitled "Anionic Activators of Photoreceptor Cells in the Dark" and the second entitled "Visualization of Actin in Photoreceptor Cells by Light Microscopy".

Finally, a special highlight of the year was the opportunity to spend 10 days at LAIR during the summer of 1983. It was a most profitable period which strengthened the strong interactions that have developed between my laboratory and Col. Beatrice's excellent program in

ocular hazards at LAIR. A report on this visit was included in our July quarterly report.

II. Anionic Activators of Photoreceptor Cells in the Dark

A. Introduction

Vertebrate retinal rod outer segments (ROS) contain a light-activated phosphodiesterase (PDE) that is highly specific for cyclic GMP (1-6). Photoexcited rhodopsin does not bind to PDE directly, but activates this enzyme via an intermediary protein called the G-protein or transducin (7). The absorption of light induces a conformational change in rhodopsin that results in the binding of the G-protein to rhodopsin (8) and the catalytic exchange of GTP for GDP on the G_α subunit of the G-protein (7). G_α-GTP dissociates from rhodopsin and the $G_{\beta\gamma}$ complex, and binds to phosphodiesterase (7). The binding of G_α-GTP to PDE results in the dissociation of the inhibitory γ subunit of phosphodiesterase with the subsequent hydrolysis of cyclic GMP to GMP (1-6). In vitro the response of this system to light is highly amplified and is associated with visual transduction, since the absorption of a single photon results in the catalytic exchange of GTP for GTP on ≈500 G-proteins (7), and these G-proteins each activate ≈800 PDE molecules leading to the hydrolysis of 4×10^5 cyclic GMP within one second of photon absorption (2).

The activation of PDE by light has many similarities to the activation of adenylate cyclase by hormone receptors located on the surface of many types of eukaryotic cells (10). The absorption of light by rhodopsin (7) and the binding of catecholamine hormones to cell surface receptors (11) both catalyze the exchange of GTP for GDP bound to the

respective G-protein of each system (10). In the adenylate cyclase system, the G-GTP complex activates the catalytic subunit of this enzyme, leading to the synthesis of cyclic AMP from ATP (11). Recently, there has been a report of a functional exchange of the components of the adenylate cyclase and ROS phosphodiesterase systems (12).

Fluoride ions (13-18) vanadate (19) and molybdate (20,21) activate membrane-bound adenylate cyclase purified from a number of different tissues, but tungstate does not activate this enzyme (20). In this paper, we demonstrate that vanadate, fluoride, molybdate and tungstate activate rod outer segment PDE in the absence of light. Since tungstate stimulates ROS PDE at low concentrations but does not activate adenylate cyclase, this anion may be employed as a selective stimulator of PDE-mediated cyclic nucleotide hydrolysis in photoreceptors and other cells.

Materials and Methods

All reagents were obtained from Sigma (St. Louis, MO) unless otherwise noted. Bovine retinas were obtained from American Stores (Lincoln, NE) and kept in liquid nitrogen until use. Retinal rod outer segments were isolated by conventional sucrose flotation techniques, with brief centrifugation times to avoid increasing the dark PDE activity (2). Isolation procedures were carried out at 4°C or with reagents on ice using infrared illumination (λ>750 nm) and an image convertor (NI-Tec, Inc., Niles, IL). Typically, 100 bovine retinas were removed from liquid nitrogen and thawed at room temperature for 30 minutes, followed by immersion of the vials in cool water for further thawing as necessary. Retinas were placed in 45% sucrose (w/v) in a buffer (60 mM

KCl, 30 mM NaCl, 2 mM $mgCl_2$, 1 mM dithiothreitol, and 10 mM HEPES at pH 7.8) and manually homogenized by four passages through a teflon-glass test tube homogenizer (Wheaton), followed by 45-60 seconds of agitation on a tabletop vortexer operated at full speed. 32 cc of this material was placed in each of 3 cellulose nitrate tubes, overlayed with 1-2 cc of the above buffer, and centrifuged at 22K for 20 minutes in an SW 25.1 swinging bucket rotor (Beckman, Palo Alto, CA). Crude ROS harvested from the sucrose-buffer interface were diluted 4:1 with buffer and centrifuged at 5K for 20 minutes in a fixed-angle SW 30 rotor (Beckman). The resulting pellet was resuspended in 96 cc of 38% sucrose (w/v) in the above buffer, divided into 3 cellulose nitrate tubes each overlayed with 1-2 cc of buffer, and centrifuged at 22K for 20 minutes as above. Purified ROS harvested from the sucrose-buffer interface were diluted 4:1 with buffer and pelleted at 5K for 20 minutes. The pellet was resuspended in several cc of buffer, divided into 200 µl aliquots, and stored in liquid nitrogen until further use. A 10 µl aliquot of this suspension was solubilized in 1 cc of 1.5% Ammonyx LO (Onyx Chemicals, Jersey City, NJ) in 10 mM HEPES, 50 mM hydroxylamine at pH 7.8, and the rhodopsin concentration was determined by absorption difference spectroscopy using ε = 42,700 M^{-1} cm^{-1} at 500 nm. A_{280}/A_{500} was typically 1.9-2.3.

Experiments were performed at room temperature by diluting the ROS suspension to a final concentration of 4-15 µM rhodopsin. The assay mixture contained 4 mM cyclic GMP and 1 mM $CaCl_2$ in the above buffer in a total volume of 250 µl. The ROS solution was placed in a small test tube and rapidly stirred with a magnetic spin bar. For dark trials,

2.5 µl aliquots of a concentrated stock solution containing the anion of interest were added to the ROS suspension at ≈1 minute intervals, with up to 8 serial additions of anion per sample. In this manner, each ROS solution could be used to determine the PDE activity at several different anion concentrations. The number of serial additions was limited by two factors: (1) all measurements were completed before the pH changed by 0.2 units, and (2) the total added volume was limited to less than 8% of the initial volume. The effect of diluting the ROS sample by up to 8% of the initial volume was corrected for by multiplying the measured rate of cyclic GMP hydrolysis by $[(250 + \alpha)/250]^2$, where α is the volume of solution (in µl) added to the ROS suspension during the course of the experiment. This theoretical correction factor takes into account the decrease in the rhodopsin concentration of the suspension, and the attenuation of the measured pH change by the larger volume of the assay solution. The validity of using this correction factor was tested experimentally by diluting the ROS sample by up to 8% with serial additions of 2.5 µl aliquots of buffer, and the theoretical correction factor was found to negligibly underestimate the experimentally determined value.

To determine the effect of these anions on the light-activated rate of cyclic GMP hydrolysis by PDE, the ROS sample was maximally activated by either full bleaching in room lights or exposure to a calibrated commercial photoflash unit (Vivitar) placed 20 cm from the sample. Either 40 µM GPPNHP or 1 mM GTP was added to the ROS suspension prior to illumination, since light activation of PDE requires a guanyl nucleotide cofactor (10). When bright flash illumination and a GTP co-

factor were used, the initial measurement of light-activated PDE activity was made 30 seconds after the flash, since we observed that the activity of PDE remains constant for several minutes after this time. The effect of the anion of interest on light-activated PDE activity was then determined by serial additions of 2.5 µl aliquots of a concentrated stock solution of this anion, as described above.

The protons released by complete hydrolysis of 4 mM cyclic GMP led to a pH change of ≈0.7 units. This change in pH was recorded by displaying the output of a portable pH meter equipped with a microelectrode (Markson Scientific, Phoenix, AZ) on a strip chart recorder. The phosphodiesterase activity (moles of cyclic GMP hydrolyzed/second) is determined by the slope of this tracing, since hydrolysis of one mole of cyclic GMP releases one mole of H^+ at pH 7.8 (4). Buffering capacities of the individual media were determined by back titration with 0.1 N NaOH.

B. Results

Vanadate is the most potent activator of ROS PDE (K_M ≈ 100 µM), and the concentration of vanadate that maximally activates PDE in the dark is 2 mM (Figure 1). Within the error of our measurements, adding 2 mM vanadate does not significantly increase the activity of light-activated PDE. Concentrations of vanadate greater than 2 mM markedly inhibit the activity of PDE activated either by light or by lower concentrations of vanadate in the dark. The K_I value for vanadate inhibition is ≈ 6 mM. Although greater than 6 mM vandate significantly increases the buffering capacity of the ROS suspension, the measured

hydrolytic velocities can readily be corrected for this effect. The inhibition of PDE activity by vanadate is unequivocal, since the decrease in hydrolytic velocity caused by > 2 mM vanadate greatly exceeds any error introduced by correcting for these buffering capacity changes. The inhibition of PDE by high concentrations of vanadate does not appear to be due to a non-specific ionic perturbation of the medium, since up to 100 mM excess NaCl inhibits the light-induced activity of PDE by less than 10% (data not shown). Fluoride exactly duplicates the results on vanadate (data not shown).

Tungstate activates PDE in the dark at higher anion concentrations than are required for vanadate or fluoride activation (Figure 2). The K_M for tungstate activation is ≈ 1 mM, and 10 mM tungstate activates PDE to nearly the same extent that this enzyme is activated by light. Up to 10 mM tungstate does not significantly increase the activity of PDE that is activated by light. Concentrations of tungstate greater than 10 mM may inhibit PDE activity stimulated either by light or by less than 10 mM tungstate in the dark. However, we cannot be certain of the inhibitory effect of this anion because the large changes in buffering capacity produced by greater than 10 mM tungstate limited the accuracy of our measurements. If tungstate inhibits PDE at high concentrations, this inhibition is not as striking as in the case of vanadate inhibition of this enzyme.

Molybdate is the least potent of these anionic activators of PDE, since the K_M for molybdate activation is ≈ 3 mM (Figure 3). 10-20 mM molybdate maximally activates PDE in the dark, but the level of PDE

activity produced by this molybdate concentration is only 30-35% of the PDE activity produced by light. 30 mM molybdate either does not inhibit or minimally inhibits PDE activated by either light or lower concentrations of molybdate. As in the case of tungstate, the change in buffering capacity produced by high concentrations of molybdate limits the accuracy with which an inhibitory effect of this anion can be determined.

Chromate, a group VI B tetroxo complex similar to vanadate, molybdate and tungstate, does not significantly activate ROS phosphodiesterase in the dark (data not shown).

In the presence of 0.5 mM ATP and 0.5 mM GTP, PDE activated by a weak flash undergoes a first order decrease in the rate of cyclic GMP hydrolysis (referred to as deactivation), with a time constant of 11-18 seconds in 10^{-9} M Ca^{++} and 28-42 seconds in 10^{-3} M Ca^{++} (6). All of the results reported in this paper on anionic activation of PDE were obtained with 10^{-3} M Ca^{++} added, to avoid any uncontrolled effects arising from small amounts of contaminating Ca^{++} in our assay. However, since flash-induced deactivation is most striking in 10^{-9} M Ca^{++}, we conducted our assay for anion-induced deactivation in low Ca^{++}. Using 10^{-9} M Ca^{++}, we observed that the phosphodiesterase activity remained constant for at least 2 minutes after addition of 1.2 mM vanadate, 0.8 mM tungstate and 2-4 mM molybdate in the presence of 0.5 mM ATP and 0.5 mM GTP in the dark. Thus, we did not obtain any evidence to suggest that anion-activated PDE undergoes an ATP-dependent deactivation similar to the ATP-dependent deactivation of PDE after a flash of light.

C. Discussion

Our results demonstrate that vanadate, fluoride, molybdate and tungstate each activate rod outer segment phosphodiesterase in the dark. Vanadate and fluoride ($K_M \approx 100$ µM) is the most potent activator of ROS PDE, followed by tungstate ($K_M \approx 1$ mM) and molybdate ($K_M \approx 3$ mM). Either 2 mM vanadate or 10 mM tungstate produces PDE activity which is > 90% of the maximal light-activated rate for this enzyme. However, 10-20 mM molybdate can elicit only 30-35% of the activity of PDE produced by light. PDE in ROS suspensions that is maximally activated by light and a guanyl nucleotide cofactor cannot be activated further by addition of vanadate, fluoride, molybdate or tungstate. High concentrations of vanadate and fluoride clearly inhibit the activity of ROS PDE elicited by either light or up to 2 mM vanadate or fluoride in the dark. High concentrations of molybdate and tungstate may also minimally inhibit PDE, but this is difficult to determine because the change in buffering capacity due to large amounts of tungstate and molybdate limited the accuracy of our measurements.

Possible Mechanism for Anionic Activation of PDE

Fluoride activates adenylate cyclase by interacting with the G-protein (15), and vanadate and molybdate may also activate this enzyme by interacting with the G-protein (21). In view of the similarities between light-activated PDE and hormone-stimulated adenylate cyclase (10,12), we would like to suggest that vanadate, fluoride, molybdate and tungstate may activate PDE by acting on the G-protein of the ROS enzyme system. Although the molecular aspects of this activation are not known, several facts suggest how these anions might stimulate ROS

PDE. The chemistry of vanadate, tungstate and molybdate oxyanions is very similar to the chemistry of phosphate (22,23). Vanadate competes with phosphate for binding, and the ability of vanadate to adopt a structure similar to the transition state of phosphate may account for its ability to inhibit a wide variety of enzymes (22,24). If the G-protein is involved in the activation of PDE by these anions, a simple and elegant mechanism to explain this effect can be suggested. Since it is known that GTP must replace GDP on the G_α subunit of the G-protein in order to stimulate PDE (7,8), the presence of the terminal γ-phosphate of GTP must be crucial for the activation of PDE by light. In the absence of GTP exchange stimulated by photolyzed rhodopsin, vanadate, molybdate and tungstate (represented as A in Figure 4) may be capable of assuming a molecular configuration that mimics the presence of the terminal γ-phosphate of GTP at the guanyl nucleotide binding site of G_α. This could result in the dissociation of G_α from $G_{\beta\gamma}$ which is required for PDE activation. Interestingly, the recent demonstration that aluminum is required for the activation of adenylate cyclase by fluoride (25,26) may allow the activation of PDE by fluoride previously reported (12,18) to be incorporated into the above scheme. Aluminum in the presence of fluoride may exist primarily as AlF_4^-, suggesting that a metal liganded with multiple fluoride ions is the species involved in activation of adenylate cyclase (25). Therefore, the activation of phosphodiesterase by fluoride may be due to the generation of a polyionic complex that can bind to the same site at which vanadate, molybdate and tungstate activate PDE.

References

1. Liebman, P. A. and Pugh, E. N., Jr. (1979) Vision Research 19, 375-380.
2. Yee, R. and Liebman, P. A. (1978) J. Biol. Chem. 253, 8902-8909.
3. Liebman, P. A. and Pugh, E. N., Jr. (1980) Nature 287, 734-736.
4. Kawamura, S. and Bownds, M. D. (1981) J. Gen. Physiol. 77, 571-591.
5. Polans, A. S., Kawamura, S. and Bownds, M. D. (1981) J. Gen. Physiol. 77, 41-48.
6. Del Priore, L. V. and Lewis, A. (1983) Biochem. Biophys. Res. Commun. 113, 317-324.
7. Fung, B. K. K. and Stryer, L. (1980) Proc. Natl. Acad. Sci. U.S.A. 77, 2500-2504.
8. Kuhn, H. (1981) in Current Topics in Membrane and Transport (Miller, W. H., ed.) Vol. 15, pp. 171-201, Academic, New York.
9. Hurley, J. B. and Stryer, L. (1982) J. Biol. Chem. 257, 11094-11099.
10. Pober, J. S. and Bitensky, M. W. (1979) Adv. Cyclic Nucleotide Res. 11, 265-301.
11. Levitsky, A. (1981) C.R.C. Critical Reviews in Biochem. 10, 81-112.
12. Bitensky, M. W., Wheeler, M. A., Rasenick, M. M. Yamazaki, A., Stein, P. J., Halliday, K. R. and Wheeler, G. L. (1982) Proc. Natl. Acad. Sci. U.S.A. 79, 3408-3412.
13. Rall, T. W. and Sutherland, E. W. (1958) J. Biol. Chem. 232, 1065-1076.

14. Howlett, A. C., Sternweiss, P. C., Macik, B. A., Van Arsdale, P. M. and Gilman, A. G. (1979) J. Biol. Chem. 254, 2287-2295.

15. Eckstein, F., Cassel, D., Levkovitz, H., Lowe, M. and Selinger, Z. (1979) J. Biol. Chem. 254, 9829-9834.

16. Downs, R. W., Jr., Spiegel, A. M., Singer, M., Reen, S. and Aurbach, G. D. (1980) J. Biol. Chem. 255, 949-954.

17. Sternweiss, P. C., Northup, J. K., Smigel, M. D. and Gilman, A. G. (1981) J. Biol. Chem. 256, 11517-11526.

18. Sitaramayya, A., Virmaux, N. and Mandel, P. (1977) Exp. Eye Res. 25, 163-169.

19. Schwabe, U., Puchstein, C. Hannemann, H. and Sochtig, E. (1979) Nature 277, 143-145.

20. Richards, J. M. and Swislocki, N. I. (1979) J. Biol. Chem. 254, 6857-6860.

21. Richards, J. M. and Swislocki, N. I. (1981) Biochim. Biophys. Acta 678, 180-186.

22. Macara, I. G. (1980) Trends in Biochemical Science 5, 92-94.

23. Pope, M. T., Still, E. R. and Williams, R. J. P. (1980) in Molybdenum and Molybdenum-containing Enzymes (Coughlan, M. P., ed.) pp. 1-40, Pergamon, Oxford.

24. Cantley, L. C., Jr., Cantley, L. G. and Josephson, L. (1978) J. Biol. Chem. 253, 7361-7368.

25. Sternweis, P. C. and Gilman, A. G. (1982) Proc. Natl. Acad. Sci. U.S.A. 79, 4888-4891.

26. Mansour, J. M., Ehrlich, A. and Mansour, T. E. (1983) Biochem. Biophys. Res. Commun. 112, 911-918.

Figure 1: Vanadate Activates Rod Outer Segment Phosphodiesterase. In the dark, low concentrations of vanadate stimulate the activity of ROS PDE, with 2 mM vanadate stimulating this enzyme to > 90% of the light-induced activity. Concentrations of vanadate > 2 mM inhibit the activity of PDE elicited by light or lower vanadate concentrations in the dark. The light curve was determined by bleaching 6% of the rhodopsin present in ROS suspensions containing 1 mM GTP as a cofactor. The effect of vanadate on the activity of PDE in ROS samples bleached in room lights was also investigated, and the results obtained were similar to the results obtained using flash illumination (results not shown). Assay mixtures contained 1 mM $CaCl_2$ and 4 mM cyclic GMP in buffer (see text). All suspensions were 10.2 μM in rhodopsin. Experiments were performed at room temperature at an initial pH of 7.8, and all measurements were completed before the pH had changed by 0.2 units. A Relative PDE Activity = 1.0 corresponds to 14.3 μM of cyclic GMP hydrolyzed/sec.

Figure 2: Tungstate Activates Rod Outer Segment Phosphodiesterase. In the dark, 10 mM tungstate stimulates the activity of ROS PDE to a level > 90% of the light-induced activity. Concentrations of tungstate greater than 10 mM may exert a slight inhibitory effect on PDE activity, but this is uncertain because of the change in buffering capacity introduced by this anion. The effect of tungstate on the light-induced activity of PDE was determined with 40 μM GPPNHP as a cofactor, and with the sample activated by a flash bleaching 0.2% of the rhodopsin present. Assay mixtures contained 1 mM $CaCl_2$ and 4 mM cyclic GMP.

Experiments were performed at an initial pH of 7.8. Suspensions were 4 μM in rhodopsin, and a Relative PDE Activity = 1.0 corresponds to 17.7 μM cyclic GMP hydrolyzed/sec.

Figure 3: Molybdate Activates Rod Outer Segment Phosphodiesterase. In the dark, 10-20 mM molybdate stimulates PDE activity to a level 30-35% of the light-induced activity of this enzyme. The effect of molybdate on the light-induced activity of PDE was determined with 1 mM GTP as a cofactor, and with the sample fully activated by bleaching in room lights. Assay mixtures contained 1 mM $CaCl_2$ and 4 mM cyclic GMP. Suspensions were 10.2 μM in rhodopsin, and experiments were performed at an initial pH of 7.8. A Relative PDE Activity = 1.0 corresponds to 11.4 μM of cyclic GMP hydrolyzed/sec.

Figure 4: Mechanism for the Anionic Activation of Phosphodiesterase. (a) In rod outer segments, the effect of light is to induce the binding of the G-protein (G) to rhodopsin (Rh), resulting in the catalytic exchange of GTP for GDP on the G-protein. G-GTP then stimulates phosphodiesterase (PDE), resulting in the hydrolysis of cyclic GMP to GMP. (b) In adenylate cyclase, the binding of hormone (H) to cell surface receptors (Rec) results in the exchange of GTP for GDP on the G-protein of this system. G-GTP then activates the catalytic subunit (C), resulting in the conversion of ATP to cyclic AMP. (a') and (b'): Anions (A) that activate both ROS PDE and adenylate cyclase may produce their effect by interacting with the G-protein of each system. Since vanadate, molybdate and tungstate may be able to assume structures similar

to the transition state of phosphate, we suggest that these oxyanions may assume a molecular configuration that mimics the presence of the terminal γ-phosphate at the guanyl nucleotide binding site on the G-protein. This could result in the activation of PDE and C by the stimulated G-protein.

Figure 1: Vanadate Activates Rod Outer Segment Phosphodiesterase

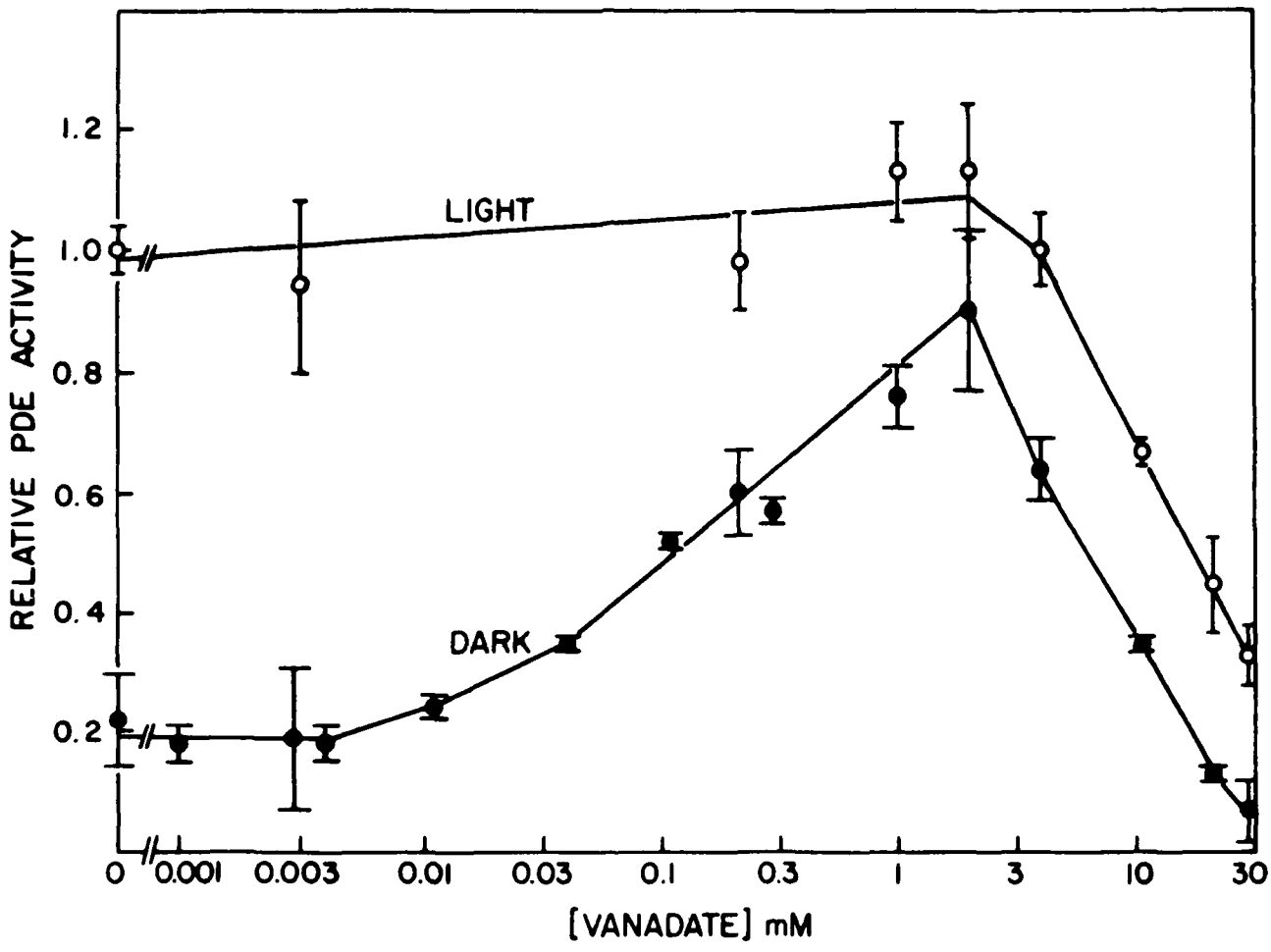

Figure 2: Tungstate Activates Rod Outer Segment Phosphodiesterase

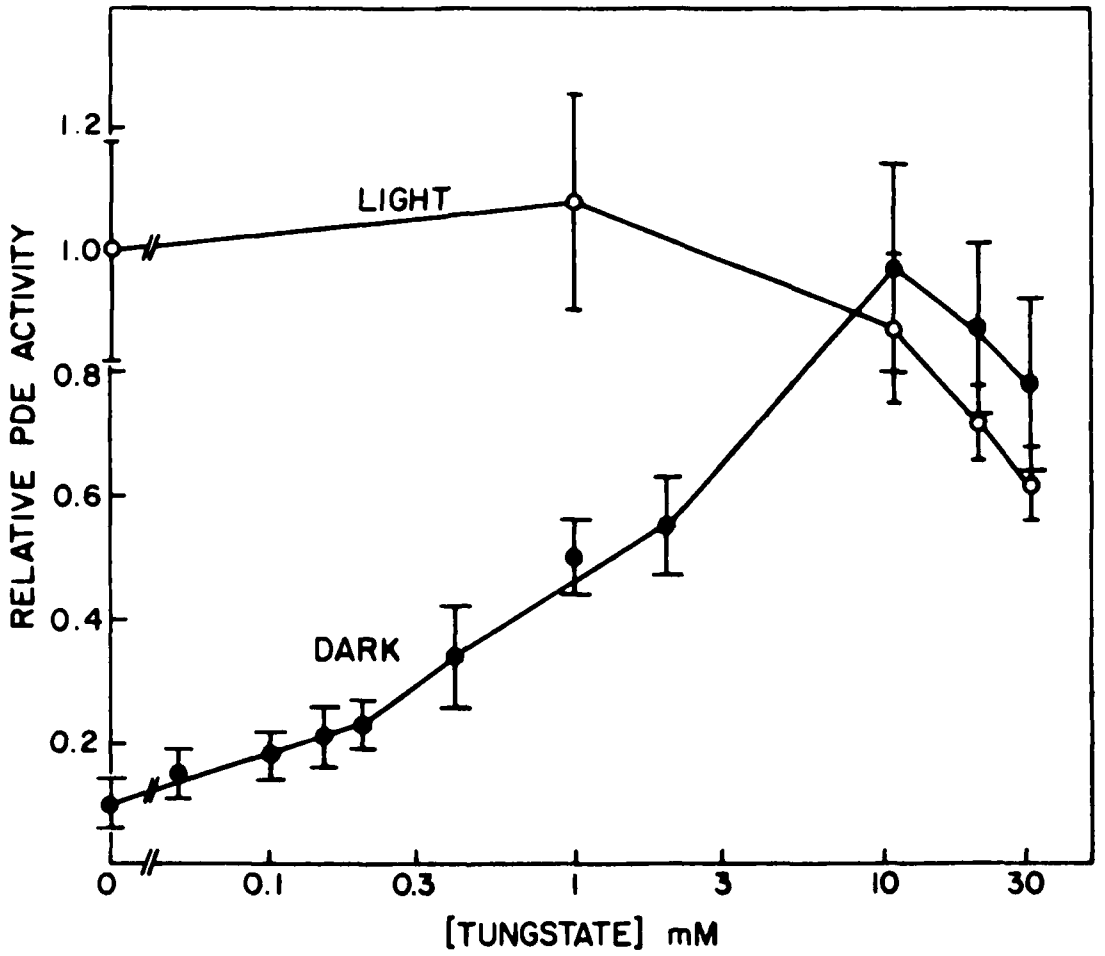

Figure 3: Molybdate Activates Rod Outer Segment Phosphodiesterase

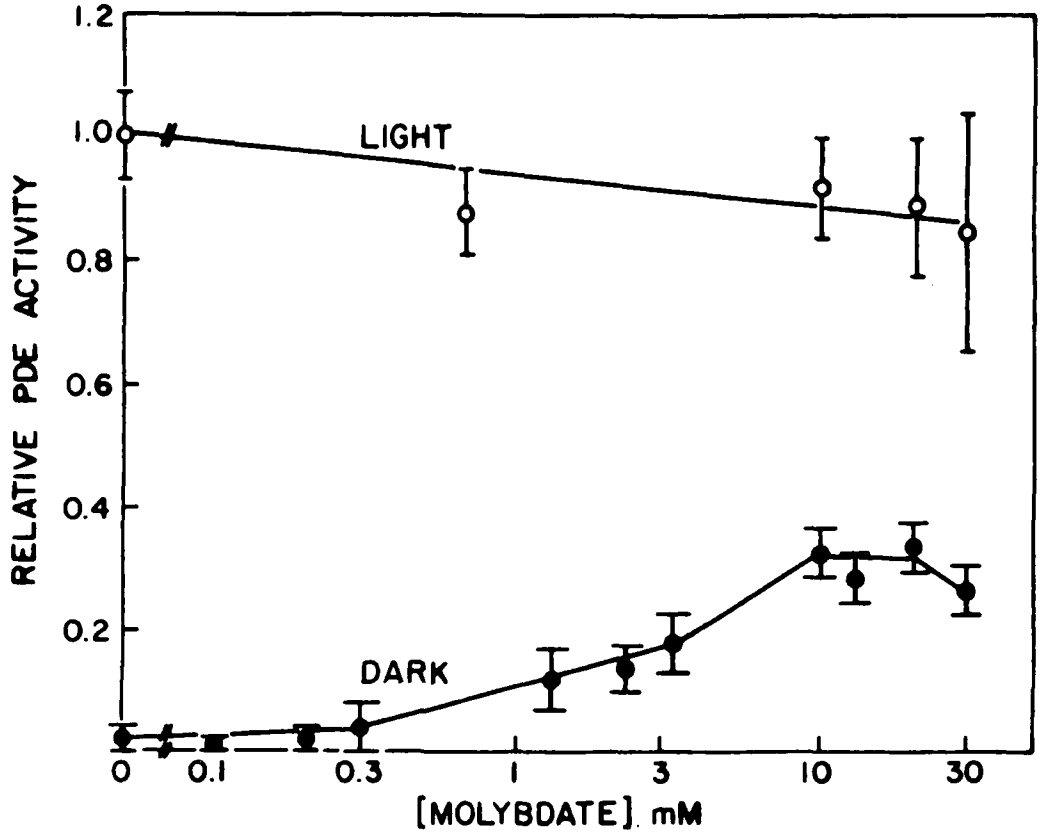

Figure 4: Mechanism for the Anionic Activation of Phosphodiesterase

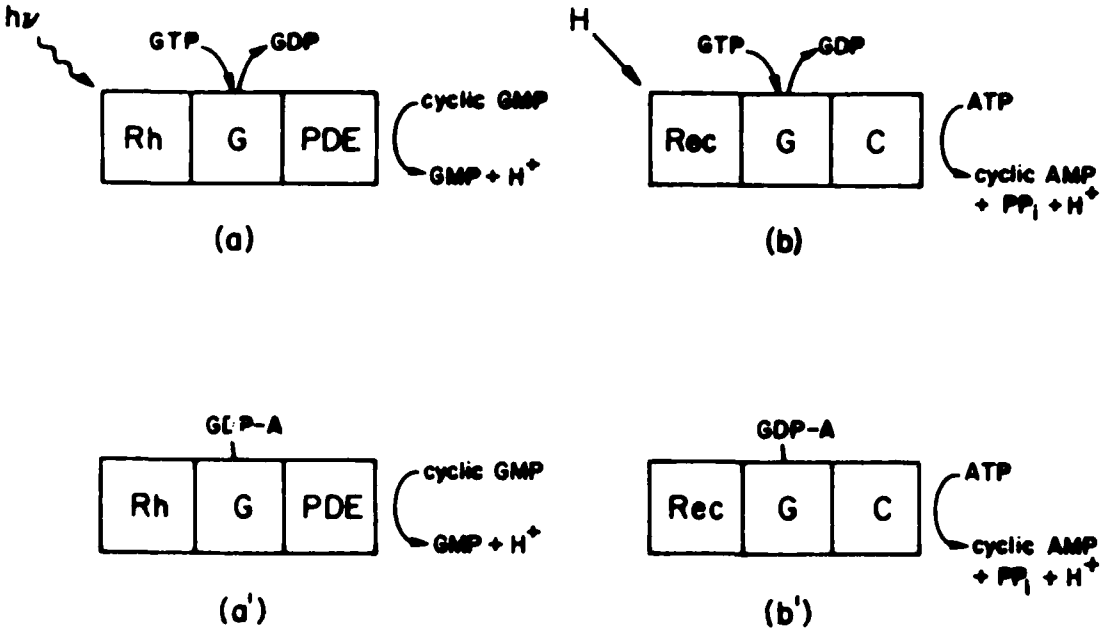

III. Visualization of Actin in Photoreceptor Cells by Light Microscopy

A. Introduction

Rod and cone photoreceptors contain actin (4-8) in the calyceal processes (1-10) surrounding the base of the outer segment. First described in Nectarus (1), the calyceal processes are finger-like projections that arise from the apex of the inner segment and surround the base of the outer segment (1-9). In rod photoreceptors that contain scalloped discs, one calyceal process lies in each surface groove corresponding to an invagination of the discs (1,2). In humans or macaque, there are 9-12 calyceal processes per ROS, and they do not appear to be closely adherent to the plasma membrane (2). As Cohen has noted, the fact that the calyceal processes do not appear to run the length of the rod cell and are loosely applied to the membrane surface in at least some species argues against a primary role for these structures in visual transduction (2).

In teleost photoreceptors, actin filaments extend from the calyceal processes surrounding the base of the outer segment to the photoreceptor pedicle (4,6). In cone cells, these filaments extend into the inner segment, the outer fiber, around the photoreceptor nucleus, and through the inner fiber prior to inserting in the plasma membrane near the synapse (4,6). Throughout their excursion, these filaments lie immediately subjacent to the plasma membrane. The distribution of actin filaments in teleost rods is very similar, with the important exception that filaments have not been documented in the perinuclear region. Therefore, in rod photoreceptors it is unclear if actin filaments in the inner fiber are continuous with filaments found in the inner segment.

Electron microscopy has previously been utilized to visualize actin filaments in rod and cone photoreceptors of many different species. However, although electron microscopy offer high structural detail and spatial resolution, this technique suffers from the limitations inherent in trying to reconstruct a three-dimensional view of actin filaments from multiple thin serial-sections. In addition, there is obviously no possibility of utilizing electron microscopy to visualize actin filaments in live photoreceptors. Lastly, using heavy meromyosin/subfragment-1 labeling procedures to identify actin raises the possibility of polymerization of ambient G-actin during the extended glycerination treatment (11).

Actin localization techniques utilizing fluorescently-labeled phallicidin circumvent these difficulties. Phallicidin is a potent toxin isolated from the fungus Amanita phalloides that selectively binds to and stabilizes F-actin in plant and animal cells (11-15). G-actin oligomers also bind phallicidin, but G-actin monomers do not. The three-dimensional arrangement of F-actin filaments in cells can be observed in the light microscope by staining these filaments with phallicidin conjugated to a fluorescent label. Brief fixation procedures, permeabilization of live cells by lysolecithin treatment and vesicle fusion techniques can all be used to introduce phallicidin into cells with a minimum amount of fixation artifact. Fluorescently-labeled phallicidin has previously been used to label actin in fixed tissue culture fibroblasts (14), live mouse myoblasts (13), algae (14), conifer roots (11), metaphase spindles in rat kangaroo cells (12) and stress fibers in vascular endothelial cells (15).

In these experiments we have used rhodamine-phallicidin (Rhod-Ph) to obtain a three-dimensional view of fluorescently-labeled actin filaments in isolated rod photoreceptors and photoreceptors attached to the retina. Our results confirm the presence of actin filaments in the calyceal processes surrounding the base of the outer segments. These filaments are continuous with longitudinally-oriented filaments that lie beneath the plasma membrane in the ellipsoid and myoid regions of the inner segment. In addition, we have localized actin at the base of the outer segment in fibers oriented perpendicular to the long axis of the rod photoreceptor.

Material and Methods

Bufo marinus toads 4-6 cm in length of either sex were obtained from Lemberger Associates(Germantown, WI). Toads dark adapted for at least 10-12 hours were decapitated and the eye globe was rapidly enucleated using either infrared illumination ($\lambda > 750$ nm) and an image convertor(Ni-Tec, West Jarvis, IL) or dim red illumination. The enucleated eye was hemisected just posterior to the ora serrata, and the retina was gently lifted away from the pigment epithelium with fine forceps. The retina was placed in 200 µl of a modified Ringer's solution (65 mM NaCl, 50 mM $NH_2OH{\cdot}HCl$, 2.5 mM KCl, 10 mM (N-2-hydroxyethylpiperazine-N'-2-ethanesulfonic acid (HEPES), 2 mm $MgCl_2$, 1 mM $CaCl_2$, 5 mM glucose, pH 7.5-7.8), and rod outer segments (ROS) were isolated by swirling the retina for 30-60 seconds. The purpose of substituting $NH_2OH.HCl$ for NaCl was to decrease the autofluorescence of outer segments arising from the photoproducts of rhodopsin (18). Retinal fragments that remained after the detachment of the outer segments

were prepared sliced into thin strips with a sharp knife with the aid of a dissecting microscope. Dim red illumination was used in this step, as the infrared image convertor was not interfaced with the dissecting microscope. Retinal fragments with outer segments attached were prepared by avoiding the ROS isolation step described above.

Some of the ROS suspensions or retinal fragements were fixed in 3.7% formaldehyde for 30-60 minutes. Unfixed ROS suspensions were permeabilized by freezing at -10°C for 20 minutes followed by thawing at room temperature. However, the morphology of the cells was inferior to the formaldehyde-fixed cells. Staining was carried out by transferring 50-100 µl of the ROS suspension or 1-2 retinal fragments to a glass slide and incubating with 50 µl of 150 ngml of fluorescently-labeled phallicidin for >20 minutes. Phallicin labeled with 7-nitrobenz-2-oxa-3 diazole(NBD)(Molecular Probes, Junction City, OR) or rhodamine demonstrated similar labeling, but rhodamine label gave superior photographs since autofluorescence from the rod cells partially obscured the fluorescence from NBD-phallicidin. Photographs were taken with a 35 mm camera(Olympus OM-2, Woodbury, NY) and a Nikon Optiphot microscope equipped with an episcopic fluorescence attachment and a mercury lamp excitation source. For Rhod-Ph, a dichroic mirror was used to select an excitation wavelength at 535-550 nm, and a 580 nm barrier filter was used to block the exciting lignt. Results were confirmed with NBD-phallicidin using an excitation wavelength of 450-480 nm and a 515 nm barrier filter for viewing.

3. Results and Discussion

Figure 1 shows a low-magnification view of formaldehyde-fixed toad rods detached by shaking the isolated retina in modified Ringer's solution. Although such preparations typically contain >90% isolated outer segments, rod cells with inner and outer segments attached were present in sufficient numbers that they could easily be located for fluorescence microscopy. Figure 2 shows fluorescence and phase contrast micrographs of five different rod cells exhibiting prominent staining of actin filaments by rhodamine-phallicidin. In some cells the filaments appeared to be associated as doublets but this was an inconsistent finding. In all photoreceptor cells that had inner segments attached, individual filaments originating at the scleral end of thecalyceal processes surrounding the base of the outer segment extended into the inner segment. The vitreal extent of these filaments was variable from cell to cell. In some photoreceptors, the filaments clearly run from the calyceal processes to the vitreal end of the inner segment myoid and end at the photoreceptor nucleus.

Actin filaments in each of these locations were not equally well-preserved by our formaldehyde fixation. The filaments with the calyceal processes and ellipsoid were exceptionally well-preserved, as they were always present in our preparations and appeared as thick lines of fluorescent stain (Figures 2-3). The appearance of the filaments in the myoid region was much more variable, ranging from thick individual filaments similar to the ellipsoid filaments to a diffuse, reticular staining pattern that probably represents disrupted filaments.

In rod cells attached to the retina, filament extending from the scleral side of the nucleus into deeper retinal layers are also evident (Figure 4). Since some of these fibers appear to make an abrupt 90° turn just scleral to the ucleus (Figure 4), we are fairly confident that these represent actin filaments within Henle's fibers, the morphological axon of rod photoreceptors (2). Staining of actin filaments within deeper retinal layers was frequently observed, and the staining pattern was highly suggestive of the presence of actinfilaments oriented transverse to the long axis of the rod cells (Figure 3). It is not clear if all of these filaments are within Henle's fibers, or if they are located within deeper retinal layers.

Outer segments detached from the retina by mechanical agitation separate from the inner segment at the thin connecting cilium. During this breaking process, it is possible for the calyceal processes to remain associated with either the inner segment or the outer segment. We frequently observed calyceal processes remaining associated with the outer segments (Figure 2). This was highly variable, however, as outer segments with no calyceal processes attached and inner segmentfragments with calyceal processes attached were also observed. The fact that calyceal processes can adhere to the outer segment after the inner segment is detached is somewhat surprising, since the calyceal processes are evaginations of the inner segment. In fact, Borwein (19) has recently observed that the calyceal processes of Rhesus monkey do not remain with the outer segments during isolation procedures. Our results suggest that the calyceal processes frequently adhere to the outer segment in Bufo marinus. The discrepancy between these two results may be due to species differences.

Our photographs suggest that the actin filaments in the inner segment are closely applied to the plasma membrane. By changing the depth of focus, we could visualize the three-dimensional orientation of these filaments as well as the curvature of the plasma membrane. In all cases, the filaments appear to follow the curvature of the plasma membrane very closely, but we cannot discern whether these filaments are superficial or deep to the plasma membrane of the inner segment. Figure 5 presents a unique view that further demonstrates that the actin filaments are located in the periphery of the inner segment. A retina with rod outer segments detached was cut into small fragments, fixed in formaldehyde, and stained with rhodamine-phallicidin. A top view of the scleral side of the retina is shown in Figure 4. The solid orange circles represent the non-labeled cytoplasm of the inner segment. The bright yellow rings of rhodamine-phallicidin labeling represent a cross-sectional view of actin filaments, and these filaments are clearly located at the periphery of the inner segment. Our observations are consistent with transmission electron micrographs indicating that the actin filaments lie immediately to the plasma membrane of the inner segment (4-8), and scanning electron micrographs demonstrating prominent ridges in the inner segment membrane that may be continuous with the calyceal processes (20).

We frequently observed a prominent actin band at the junction of the inner and the outer segment oriented transverse to the long axis of the rod cell. In several isolated rods detached at the connecting cilium, this band remained associated with the outer segment. This may correspond to the labeling of the lip-like expansion of the connecting cilium at the base of outer segments reported while this work was in

progress (11). In view of this localization of actin, Chaitin et al. (11) have suggested that this protein may be involved in disc morphogenesis and vectorial transport of opsin and other membrane proteins.

The rhodopsin-containing discs of the ROS have long been felt to be physically (2), electrically (21), and osmotically (22) isolated from the ROS plasma membrane. However, workers in two laboratories have recently demonstrated the presence of multiple filaments interconnecting the discs to one another and to the plasma membrane (16,17). Although the composition of these filaments is not known, it is possible that they may play a significant role in visual transduction (16,17,23). If the filaments are composed of F-actin, we would expect labeling of these structures by rhodamine-phallicidin. However, in experiments utilizing either formaldehyde-fixed ROS or ROS permeabilized by freezing and thawing, no labeling of these outer segment filaments was observed. While it may be argued that the autofluorescence arising from ROS (Figure 3) could easily obscure actin labeling in the outer segment, we do not believe this to be the case in our experiments. The amount of autofluorescence arising from formaldehyde-fixed ROS in hydroxylamine was highly variable, and on occasion no detectable autofluorescence was observed. For example, in Figure 3 there is no background fluorescence emanating from the outer segment, and no labeling of the ROS by rhodamine-phallicidin.

For several reasons, we are certain that Rhod-Ph was able to enter the outer segment under our experimental conditions: (1) the intracellular actin present in the calyceal processes and the inner segment were heavily labeled by Rhod-Ph; (2) whole rod cells with clear breaks in the plasma membrane (see Figure 4) do not demonstrate labeling with

Rhod-Ph in the vicinity of the break; and (3) short, broken outer segment fragments do not show any Rhod-Ph labeling at the apical end of the cell. Therefore, either the filaments observed in ROS (16,17) are not composed of F-actin, or these filaments are not well-preserved by our fixation procedures. Burnside and coworkers have previously noted that although the calyceal and ellipsoid filaments were well-preserved, rod myoid filaments were easily disrupted and often could not be observed in fixed photoreceptors. These myoid filaments also showed variable preservation in our own experiments. The fact that we observed these labile myoid actin filaments decreases the probability that the disc-to-disc and disc-to-membrane filaments are composed of F-actin but were not well-preserved in our preparations. However, we cannot completely rule out the possibility that these filaments are actin and were not observed with our techniques.

Summary

We have utilized rhodamine-phallicidin to visualize actin in toad rod photoreceptors by fluorescence microscopy. Actin within the calyceal processes surrounding the base of the outer segment allow these structures to be viewed by light microscopy for the first time. In toads, the calcyceal processes frequently adhere to the plasma membrane at the base of outer segments that have been detached from the inner segment at the connecting cilium. Actin filaments clearly extend from the calyceal processes to the photoreceptor nucleus, and another series of filaments are observed in the inner fiber. We do not have any evidence suggesting that the actin filaments in the myoid are continuous with the filaments within the photoreceptor axon, although this is

apparently the case in cone photoreceptors of teleost. We have also observed staining in deeper retinal layers of actin filaments oriented transverse to the long axis of photoreceptors; this may be due to actin located in photoreceptor inner fibers. Lastly, the cross-sectional photograph of the neural retina with outer segments detached shown in Figure 4 provides a unique view of actin filaments peripherally located in the photoreceptor inner segments.

Our results provide a technique for visualizing the three-dimensional structure of actin filaments in photoreceptors by light microscopy copy with a minimum of sample preparation. In addition, it should be possible to apply these fluorescent labeling techniques to living cells. Phallicidin can be introduced into live animal cells by permeabilizing the plasma membrane with lysolecithin (14) or by pinocytosis (13). Since fluorescent dye can be introduced into rod cells by vesicle fusion (20), it is possible that actin can be fluorescently labeled by these techniques in intact functioning photoreceptors.

Lastly, we have observed no labeling of the outer segment to suggest that the filaments observed by electron microscopy (16,17) connecting adjacent discs to discs to the plasma membrane are composed of F-actin. However, we cannot completely rule out the possibility that the filaments are exceptionally labile under our fixation procedures. We are presently investigating this possibility.

References

1. Brown, P. K., Gibbons, I. R. and Wald, G. (1963) J. Cell Biol. 19, 79-106.

2. Cohen, A. I. (1969) in The Retina:Morphology, Function, and Clinical Characteristics (Straatsma, B. R., Hall, M. O., Allen, R. A. and Crescitelli, F., eds.) pp. 31-62, Univ. of California, Berkeley and Los Angeles, 1969.

3. Cohen, A. I. (1961) Exp. Eye Res. 1, 128-136.

4. Burnside, B., Smith, B., Nagata, M. and Porello, K. (1982) J. Cell Biol. 92, 199-206.

5. O'Connor, P. and Burnside, B. (1982) J. Cell Biol. 95, 445-452.

6. Burnside, B. (1978) J. Cell Biol. 78, 227-246.

7. O'Connor, P. and Burnside, B. (1981) J. Cell Biol. 89, 517-524.

8. Porrello, K., Cande, W. Z. and Burnside, B. (1983) J. Cell Biol. 96, 449-454.

9. Cohen, A. I. (1965) Anat. Rec. 152, 63-80.

10. Chaitin, M. H., Schneider, B. G., Hall, M. O. and Papermaster, D. (1983) Inv. Ophth. Vis. Sci. (Supplement), 287.

11. Pesacreta, T., Carley, W. F., Webb, W. W. and Parthasarathy, M. V. (1982) Proc. Natl. Acad. Sci. U.S.A. 79, 2898-2901.

12. Barak, L. S., Nothnagel, E., DeMarco, E. F. and Webb, W. W. (1981) Proc. Natl. Acad. Sci. U.S.A. 78, 3034-3038.

13. Barak, L. S., Yocum, R. R. and Webb, W. W. (1981) J. Cell Biol. 89, 368-372.

14. Barak, L. S., Yocum, R. R., Nothnagel, E. and Webb, W. W. (1980) Proc. Natl. Acad. Sci. U.S.A. 77, 980-984.

15. Wong, A. J., Pollard, T. D. and Herman, I. M. (1983) Science 219, 867-869.

16. Usukura, J. and Yamada, E. (1981) Biomedical Res. 2, 177-193.

17. Roof, D. J. and Heuser, J. E. (1982) J. Cell Biol. 95, 487-500.

18. Hagins, W. A. and Jennings, W. H. (1959) Discussion Faraday Soc. 27, 180-190.

19. Borwein, B. (1983) Anat. Rec. 205, 363-373.

20. Yoshikami, S., Robinson, W. E. and Hagins, W. A. (1974) Science 185, 1176-1179.

21. Hagins, W. A. and Ruppel, H. (1971) Fed. Proc. 30, 64-68.

22. Korenbrot, J. I., Brown, D. T. and Cone, R. A. (1973) J. Cell Biol. 56, 389-398.

23. Del Priore, L. and Lewis, A. (1983) manuscript in preparation.

Figure 1: Low magnification view of formeldehyde-fixed toad rod photoreceptor 30-60 minutes after isolation.

Figure 2: Phase contrast (upper) and fluorescence microscopy (lower) of fixed toad photoreceptors stained with rhodamine-phallicidin. The calyceal processes surrounding the base of this truncated outer segment appear to be associated as doublets, although this was an inconsistent finding from cell to cell. Actin staining is evident as a thick band at the right margin of the nuclus (compare upper and lower photographs).

Figure 3: Phase(upper) and fluorescence (lower) micrographs of fixed toad rod outer segments. In the lower photograph, note the transverse band of actin staining at the base of the outer segment. Also note that a portion of the outer segment was broken during the isolation procedure (upper photo), and that there is no staining of the region of the outer segment at the margins of this break by rhodamine-phallicidin. This suggests that (1) there is no actin in the bulk of the outer segment, or (2) any F-actin present is extremely liabile to the fixation procedures employed.

Figure 4: These toad rod outer segments are clearly detached from the inner segment by breakage at the connecting cilium. The point of this photo is to demonstrate that the calyceal processes can remain associated with the plasma membrane of the outer segment after the inner segment has been removed.

Figure 5: Toad rod photoreceptor attached to the retina: These photos clearly demonstrate the staining of actin filaments in the calyceal processes (of stain) and inner segment. The vertical line at the extreme right of the lower photo may represent actin within the photoreceptor inner fiber.

Figure 6: Cross-sectional view of the scleral side of a fixed, stained retina with photoreceptor outer segments detached. Diffuse orange is due to retinal autofluorescence, and the bright yellow rings represent circle of actin peripherally located in the photoreceptor inner segment.

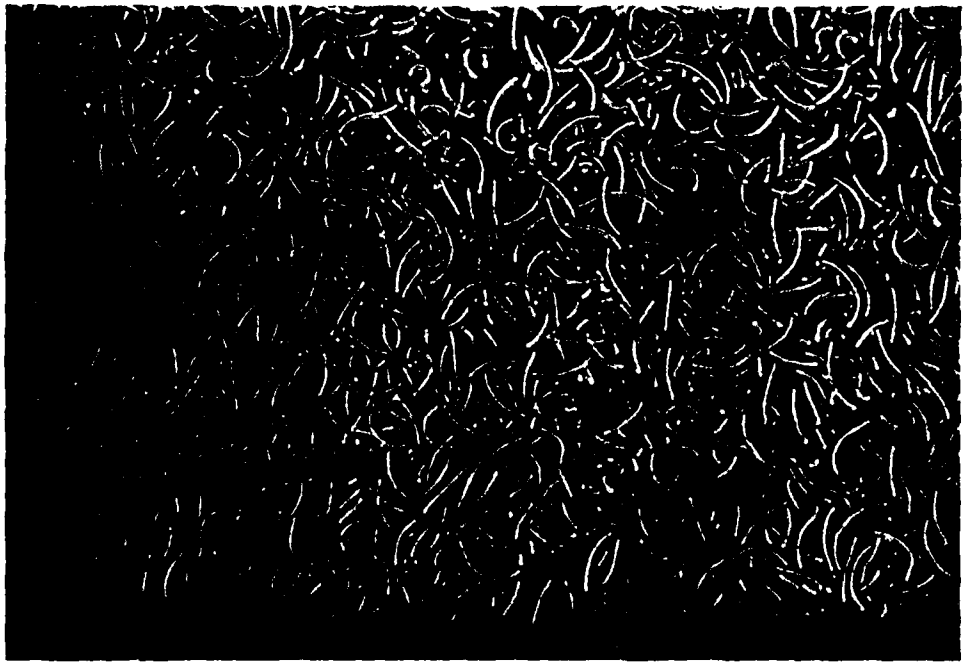

Figure 1

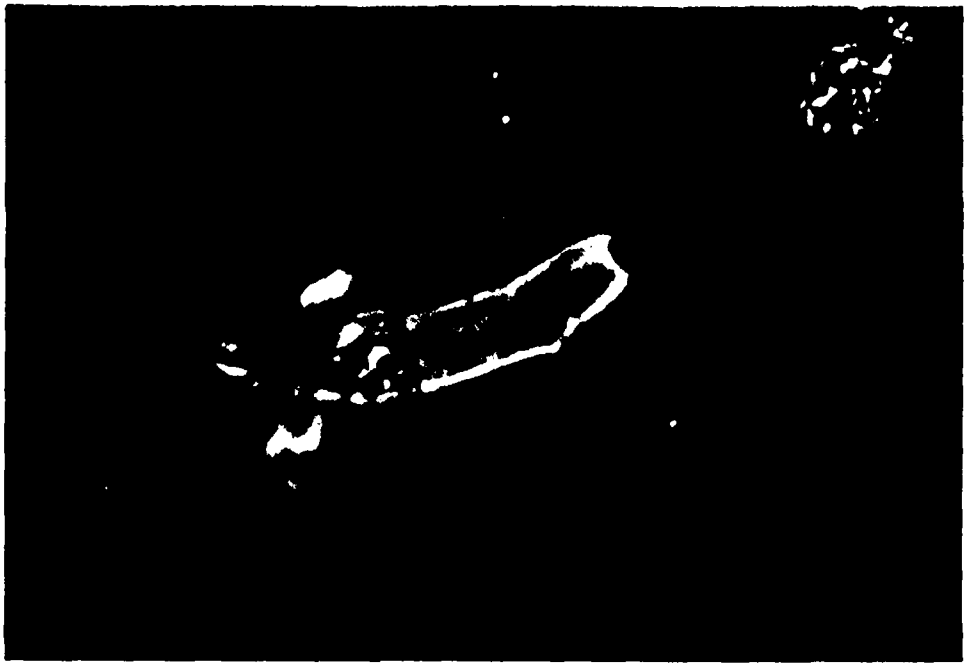

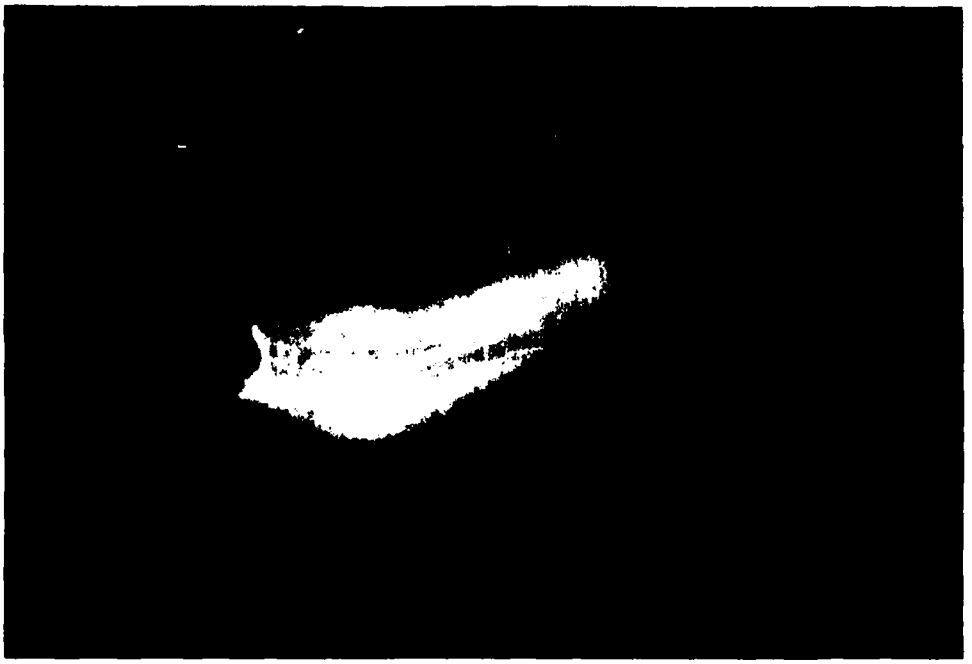

Figure 2

Figure 3

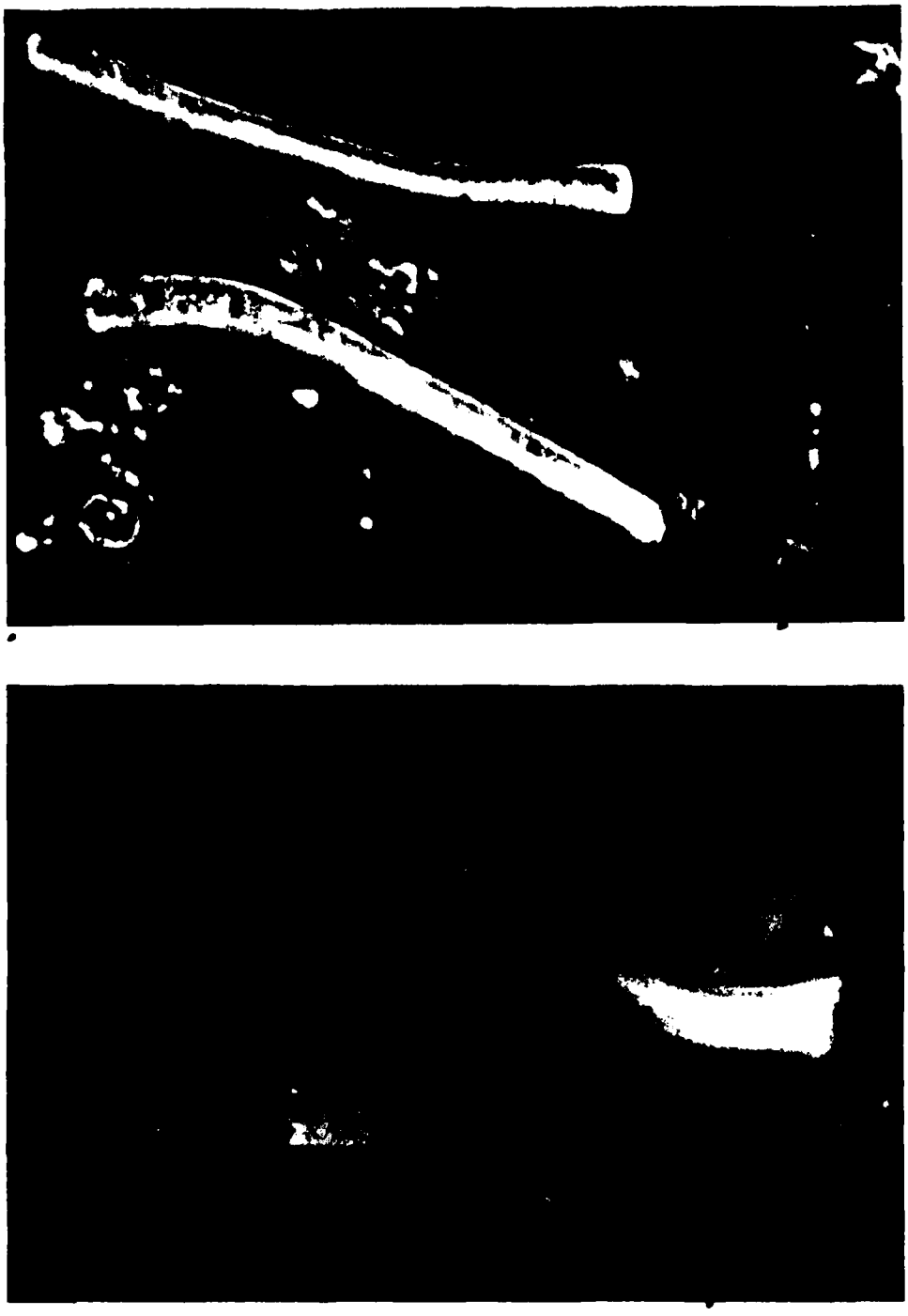

Figure 4

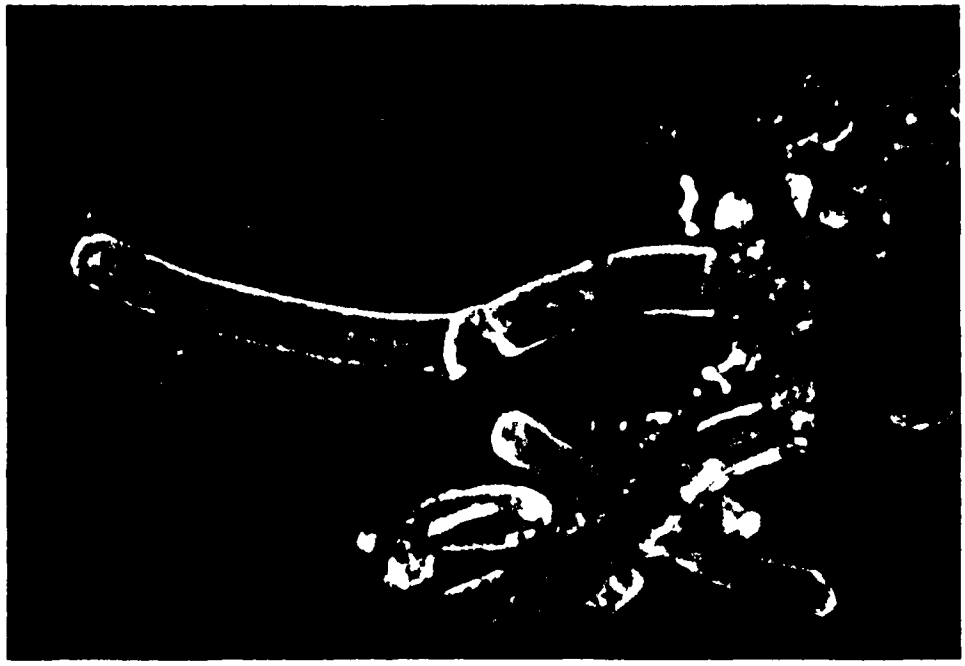

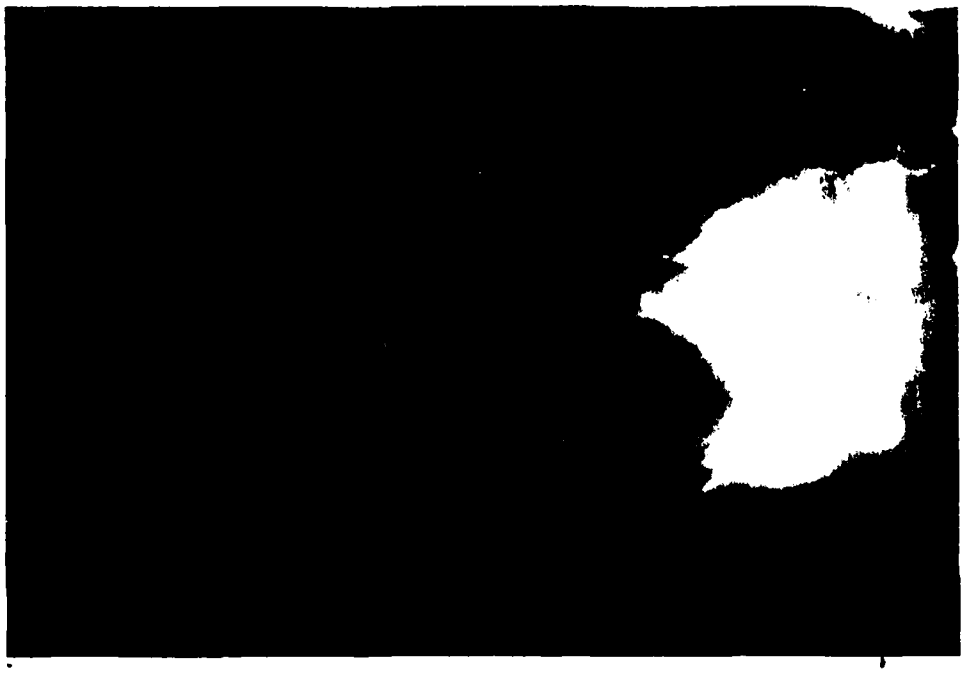

Figure 5

Figure 6

END

DTIC

11-86